Photoionization of quasi-two-electron atoms dominated by the doubly excited autoionization states

T. N. Chang
Department of Physics, University of Southern California, Los Angeles, California 90089-0484
(Received 30 October 1987)

A theoretical procedure based on the configuration-interaction approach of Fano [Phys. Rev. **124**, 1866 (1961)] is presented for the photoionization between states dominated by strong configuration interaction. By correctly identifying the main contributing interaction between the dominating bound configurations, the effectiveness of this procedure is demonstrated by its application to photoionization from the Mg $3s3p\ ^1P$ excited state to the ^1S continuum dominated by the $3p^2\ ^1S$ doubly excited autoionization state above the first ionization threshold. In addition to the good agreement with the experimental data, the individual contributions from different physical processes are also examined in detail.

I. INTRODUCTION

One of the most interesting features in the spectra of quasi-two-electron systems with two electrons outside a ^1S core, such as the alkaline-earth-metal atoms, is the presence of the strongly energy-dependent doubly excited autoionization structure above the first ionization threshold. A recent multistep, multicolor photoionization experiment,[1] similar to an earlier photoelectron study,[2] has opened up the possibility of systematic high-resolution study of the line profile of the autoionization structures corresponding to various final-state symmetries and thus complemented the more conventional experiments with electrons[3] or other radiation sources[4] in the shorter-wavelength region. Physical interpretation of such structure based on an analytical approach in terms of the configuration interaction due to doubly excited states embedded in the background ionization open channel was first introduced by Fano.[5] Numerical applications of the Fano procedure have been used to study the photoionization of alkaline-earth-metal atoms with varying degrees of success.[6,7]

One of the most important advantages of Fano's approach to the photoionization process dominated by the doubly excited autoionization state is its ability to calculate separately the strong and smooth energy-dependent parts of the transition amplitude. However, more extensive numerical applications of the Fano procedure have been hindered by two seemingly minor, but in practice important, considerations. First, in a straightforward application of the Fano procedure, the doubly excited bound component of the state wave function is coupled to the entire background open channel through a rediagonalization procedure by adding a second-order perturbation contribution to the initial Hamiltonian matrix. This second-order contribution is sometime insufficient especially when the configuration interaction between the doubly excited bound component and part of the bound components in the background open channel is strong. Second, the computational effort required is enormous in a straightforward application of the Fano procedure such as the one employed by Bates and Altick[6] when a large number of configurations are needed to ensure numerical convergence.

In this paper, a modified Fano procedure which circumvents the difficulties discussed above will be presented. More specifically, instead of treating perturbatively the interaction between the doubly excited bound component and the entire bound components of the background open channel, at least the dominant part of this interaction will be included directly in a multiconfiguration doubly excited bound component of the state wave function through a nonperturbative superposition of configuration wave-functions (SCW) procedure.[8-10] As a result the reduced interaction strength between the doubly excited bound component and the remaining background open channel can be taken into account adequately by the second-order perturbation contribution. In addition, a numerical procedure which requires much less computational effort and which was employed in our recent studies[8,9] has made a systematic quantitative estimation of photoionization dominated by the doubly excited autoionization states possible.

II. THEORY

In this section we will outline some of the important elements of the calculational procedure for the photoionization of a quasi-two-electron atom (e.g., the alkaline-earth-metal atoms) from an initial $(nsn_il_i)^{2S+1}L_i$ state to a final $(ns\varepsilon l)^{2S+1}L$ continuum dominated by a series of $(npn_fl_f)^{2S+1}L$ doubly excited autoionization states converged to the np series limit. The initial $^{2S+1}L_i$ state dominated by the nsn_il_i configuration is represented by a multiconfiguration state wave function Φ_i calculated with a nonrelativistic SCW procedure employed in our recent studies of the term values and the oscillator strength for states below the first ionization threshold.[8,10,11] Following the theoretical procedure of Fano,[5] the final ^{2S+1}L state, characterized by a doubly excited autoionization state embedded in the $nsm(\varepsilon)l$ background open channel, is represented by a state wave function[9]

$$\Psi_E = \sum_{m,l}{}' a_{ml}(E)\psi^{SL}_{nsml} + \int d\varepsilon\, a_{\varepsilon l}(E)\psi^{SL}_{ns\varepsilon l} + \sum_{\nu,\mu} f_{\nu\mu}(E)\Phi_{\nu\mu} , \quad (1)$$

where the expansion coefficients $a_{m(\varepsilon)l}$ and $f_{\nu\mu}$ are functions of energy E. The first two expansion terms over the single-configuration wave function $\psi^{SL}_{nsm(\varepsilon)l}$ [defined by Eq. (3) of Ref. 8] represent the contribution from the ^{2S+1}L background $nsm(\varepsilon)l$ open channel to the state wave function Ψ_E. As we pointed out earlier, part of the bound components in the background open channel which interact strongly with the doubly excited bound components of the autoionization states are excluded from the primed sum in the first term but included as parts of the multiconfiguration bound components $\Phi_{\nu\mu}$ in the last expansion term in Eq. (1). The multiconfiguration bound components $\Phi_{\nu\mu}$ corresponding to the dominating configuration $n_\nu l_\nu n_\mu l_\mu$ are calculated with the same SCW procedure[8,10,11] employed in the calculation of the initial state Φ_i, i.e.,[11]

$$\Phi_{\nu\mu} = \sum_{n_1,l_1,n_2,l_2} C^{SL}_{\nu\mu}(n_1l_1n_2l_2)\psi^{SL}_{n_1l_1n_2l_2} , \quad (2)$$

where $C^{SL}_{\nu\mu}(n_1l_1n_2l_2)$ represents the expansion coefficient and the configurations included in the first expansion term in Eq. (1) are excluded from the sum over $n_1l_1n_2l_2$. By replacing the single-configuration wave function $\psi_{n_\nu l_\nu n_\mu l_\mu}$ with the more realistic multiconfiguration bound component $\Phi_{\nu\mu}$ in the last expansion term in Eq. (1), the number of states required in the numerical calculation are reduced substantially. More detailed discussion on the expansion in terms of different components in Eq. (1) will be given later when the present procedure is applied to the specific photoionization process.

Similar to our earlier calculations,[8-11] the configurations included in our calculation are limited to those with two outermost electrons in various orbitals outside a ^1S frozen core of $N-2$ electrons. Such a choice of configurations has effectively excluded the contribution from the core polarization interaction, which, in principle, can be included explicitly in the numerical calculation if electronic configurations corresponding to simultaneous excitation of one outer electron and one inner shell electron from the ^1S core are also present in the calculation of the multiconfiguration state wave functions. Instead, in the present calculation, the core polarization interaction is approximated by adding to the N-particle nonrelativistic Hamiltonian $\hat{H}$ [i.e., Eq. (1) in Ref. 8] the dipole polarization potential V_α and the dielectronic potential[12] V_d, i.e.,

$$V_\alpha = -\sum_{i=1}^{N} V_p(r_i) , \quad (3)$$

$$V_d = -2\sum_{\substack{i,j \\ (i\neq j)}}^{N} (\hat{\mathbf{r}}_i\cdot\hat{\mathbf{r}}_j)[V_p(r_i)V_p(r_j)]^{1/2} , \quad (4)$$

and

$$V_p(r) = \frac{\alpha}{r^4}[1-e^{-(r/r_0)^6}] , \quad (5)$$

where α is the static dipole polarizability for the ^1S ionic core and r_0 is the fitted cutoff radius. The value of r_0 is determined by setting the energy correction Δ_{nl} due to the dipole polarization interaction, i.e.,

$$\Delta_{nl} = -\langle \chi_{nl} \mid V_p \mid \chi_{nl} \rangle \quad (6)$$

for the np orbital equal to the difference between the calculated orbital energy ε_{np} and the experimental np series limit.

In calculating the multiconfiguration wave functions $\Phi_{\nu\mu}$, the radial eigenfunctions χ of the one-particle Hartree-Fock Hamiltonian $h^{\rm HF}$ [i.e., Eq. (9) of Ref. 8] are chosen for all single configuration wave functions. For the background $nsm(\varepsilon)l$ open channel, the same one-particle Hartree-Fock radial wave function is used for the ns orbital. As for the $m(\varepsilon)l$ orbital, the radial wave function $\chi_{m(\varepsilon)l}$ is calculated with the one-particle screening Hamiltonian h_l, i.e.,

$$h_l\chi_{m(\varepsilon)l} = \varepsilon_{m(\varepsilon)l}\chi_{m(\varepsilon)l} , \quad (7)$$

where

$$h_l = h_l^{\rm HF} + (1-P_l)[V^l(r) - V_p(r) - 2\delta_{l1}(-1)^{S+L+l} \times \eta_1(0ll0;L)V_{\rm diel}(r)] \quad (8)$$

and the electron in the $\chi_{m(\varepsilon)l}$ orbital is subject to the screening potential V^l [i.e., Eq. (11) of Ref. 8 with $n_il_i = ns$] due to the electron in the ns orbital. The radial interaction $V_{\rm diel}$ corresponding to the dielectronic interaction is given by

$$V_{\rm diel}(r)\chi_{m(\varepsilon)l}(r) = [V_p(r)]^{1/2}\chi_{ns}(r)\langle \chi_{ns} \mid V_p^{1/2} \mid \chi_{m(\varepsilon)l} \rangle \quad (9)$$

and the angular factor η is given by

$$\eta_k(l_1l_2l_3l_4;L) = (-1)^{l_2-l_1+k+L}(l_1\|C^{(k)}\|l_3)(l_2\|C^{(k)}\|l_4) \times \begin{Bmatrix} l_1 & l_2 & L \\ l_4 & l_3 & k \end{Bmatrix} , \quad (10)$$

where the reduced matrix element of the spherical harmonics $C^{(k)}$ is given by[13]

$$(l\|C^{(k)}\|l') = (-1)^l[(2l+1)(2l'+1)]^{1/2} \times \begin{bmatrix} l & k & l' \\ 0 & 0 & 0 \end{bmatrix} . \quad (11)$$

All radial wave functions $\chi_{m(\varepsilon)l}$ are orthogonal to each other with the help of the projection operator P_l.

This choice of one-particle radial wave functions is necessary so that the matrix elements of the effective N-particle total Hamiltonian

$$H_t = \hat{H} + V_\alpha + V_d \quad (12)$$

will satisfy the required expressions for the application of the Fano procedure, i.e.,[9]

$$\langle \Phi_{\nu\mu} \mid H_t \mid \Phi_{\alpha\beta} \rangle = \delta_{\nu\alpha}\delta_{\mu\beta}\varepsilon_{\nu\mu} , \quad (13)$$

$$\langle \Phi_{\nu\mu} \mid H_t \mid \psi_{nsm(\varepsilon)l} \rangle = V_{\nu\mu,m(\varepsilon)l} , \quad (14)$$

$$\langle \psi_{nsml} \mid H_t \mid \psi_{nsm'l} \rangle = \delta_{mm'}(I_{ns} + \varepsilon_{ml}) , \tag{15}$$

$$\langle \psi_{nsml} \mid H_t \mid \psi_{ns\varepsilon l} \rangle = 0 , \tag{16}$$

$$\langle \psi_{ns\varepsilon l} \mid H_t \mid \psi_{ns\varepsilon' l} \rangle = \delta(\varepsilon - \varepsilon')(I_{ns} + k^2) , \tag{17}$$

where $\varepsilon_{\nu\mu}$ is the energy eigenvalue corresponding to the multiconfiguration wave function $\Phi_{\nu\mu}$ with the energy of the ground state of the ^1S ionic core set equal to zero and ε is the kinetic energy of the ionized electron given by $\varepsilon = k^2 = \varepsilon_{\nu\mu} + I_{ns}$, where $I_{ns} = \varepsilon_{ns} + \Delta_{ns}$ is the energy of the ns series limit. The present procedure follows more closely to Fano's original approach than that of Bates and Altick[6] as the Hamiltonian in the present treatment is already diagonal with respect to the multiconfiguration wave functions $\Phi_{\nu\mu}$, as shown by Eq. (13).

The expansion coefficients a_{ml} and $a_{\varepsilon l}$ in Eq. (1) can be expressed in terms of the coefficients $f_{\nu\mu}$, i.e.,[5]

$$a_{ml}(E) = [E - (I_{ns} + \varepsilon_{ml})]^{-1} \sum_{\nu,\mu} f_{\nu\mu}(E) V_{\nu\mu,ml} , \tag{18}$$

$$a_{\varepsilon l}(E) = \left[\frac{1}{E - (I_{ns} + \varepsilon)} + z(E)\delta(E - (I_{ns} + \varepsilon)) \right] \times \sum_{\nu,\mu} f_{\nu\mu}(E) V_{\nu\mu,\varepsilon l} , \tag{19}$$

whereas the expansion coefficient $f_{\nu\mu}$ satisfies the equation

$$\sum_{\nu',\mu'} U_{\nu\mu,\nu'\mu'}(E) f_{\nu'\mu'}(E) + z(E) \sum_{\nu',\mu'} W_{\nu\mu,\nu'\mu'}(E) f_{\nu'\mu'}(E) = (E - \varepsilon_{\nu\mu}) f_{\nu\mu}(E) , \tag{20}$$

where U is the second-order perturbation contribution to the interaction energy between the multiconfiguration bound components $\Phi_{\nu\mu}$ and the portion of the background open channel $nsm(\varepsilon)l$ included in the first two terms of Eq. (1), i.e.,[9]

$$U_{\nu\mu,\nu'\mu'}(E) = \sum_{m,l}{}' \frac{V_{\nu\mu,ml} V_{ml,\nu'\mu'}}{E - (I_{ns} + \varepsilon_{ml})} + \int d\varepsilon \frac{V_{\nu\mu,\varepsilon l} V_{\varepsilon l,\nu'\mu'}}{E - (I_{ns} + \varepsilon)} , \tag{21}$$

and W is a measure of the strength of the configuration interaction given by

$$W_{\nu\mu,\nu'\mu'}(E) = V_{\nu\mu,\varepsilon_0 l} V_{\varepsilon_0 l,\nu'\mu'} \tag{22}$$

where $\varepsilon_0 = E - I_{ns} = k_0^2$ and the radial wave function $\chi_{\varepsilon l}$ is normalized according to the asymptotic expression

$$\chi_{\varepsilon l} \underset{r\to\infty}{\longrightarrow} (\pi k)^{-1/2} \sin[kr + (1/k)\ln(2kr) - \tfrac{1}{2} l\pi + \delta_l] . \tag{23}$$

Numerically, the U matrix is calculated by evaluating the integral

$$U_{\nu\mu,\nu'\mu'}(E) = \langle F^l_{\nu\mu}(r) \mid G^l_{\nu'\mu'}(r) \rangle , \tag{24}$$

where

$$F^l_{\nu\mu}(r) = \sum_{n_1,l_1;n_2,l_2} C^{SL}_{\nu\mu}(n_1 l_1, n_2 l_2) \xi^{SL}_l(n_1 l_1, n_2 l_2; r) \tag{25}$$

and

$$\xi^{SL}_l(n_1 l_1, n_2 l_2; r) = (-1)^{l_2} \left[\sum_k (-1)^L \begin{Bmatrix} l_1 & l_2 & L \\ l & 0 & k \end{Bmatrix} (l \| V^k(\chi_{ns}, \chi_{n_1 l_1}; r) \| l_2) \chi_{n_2 l_2}(r) + \sum_k (-1)^S \begin{Bmatrix} l_1 & l_2 & L \\ 0 & l & k \end{Bmatrix} (l \| V^k(\chi_{ns}, \chi_{n_2 l_2}; r) \| l_1) \chi_{n_1 l_1}(r) \right] , \tag{26}$$

where the interaction $(l \| V^k \| l')$ is a function of r defined in Ref. 8. The sum in Eq. (25) covers all configurations included in Eq. (2). The one-particle radial function $G^l_{\nu\mu}(r)$ is the solution of the inhomogeneous equation

$$(\varepsilon_0 - h_l) G^l_{\nu\mu}(r) = F^l_{\nu\mu}(r) , \tag{27}$$

which can be solved by the procedure we have developed earlier.[14] We also note that with $F^l_{\nu\mu}$ defined by Eq. (25), the interaction matrix $V_{\nu\mu,m(\varepsilon)l}$ is given conveniently by

$$V_{\nu\mu,m(\varepsilon)l} = \langle F^l_{\nu\mu} \mid \chi_{m(\varepsilon)l} \rangle . \tag{28}$$

The expansion coefficient $f_{\nu\mu}$ and the function $z(E)$ are determined by the normalization condition

$$\langle \Psi_{E'} \mid \Psi_E \rangle = \delta(E' - E) . \tag{29}$$

A straightforward derivation following Fano's approach will lead to

$$\delta(E' - E)[\pi^2 + z(E)^2] \sum_{\nu,\mu;\nu',\mu'} f_{\nu\mu}(E') W_{\nu\mu,\nu'\mu'} \times f_{\nu'\mu'}(E) = \delta(E' - E) \tag{30}$$

and eventually the expressions for $z(E)$ and $f_{\nu\mu}(E)$, i.e.,

$$z(E)=\left[\sum_{\gamma,\tau}\frac{|V'_{\varepsilon_0 l,\gamma\tau}|^2}{E-\varepsilon_{\gamma\tau}(E)}\right]^{-1}, \tag{31}$$

$$f_{\nu\mu}(E)=\frac{z(E)}{[\pi^2+z(E)^2]^{1/2}}\zeta_{\nu\mu}(E), \tag{32}$$

where

$$\zeta_{\nu\mu}(E)=\sum_{\gamma,\tau}\frac{A_{\gamma\tau,\nu\mu}(E)V'_{\varepsilon_0 l,\gamma\tau}}{E-\varepsilon_{\gamma\tau}(E)}, \tag{33}$$

$$V'_{\varepsilon_0 l,\gamma\tau}(E)=\sum_{\nu,\mu}V_{\nu\mu,\varepsilon_0 l}A_{\gamma\tau,\nu\mu}(E). \tag{34}$$

The energy eigenvalue $\varepsilon_{\gamma\tau}$ is obtained in a second diagonalization of the matrix

$$U'_{\nu\mu,\nu'\mu'}(E)=U_{\nu\mu,\nu'\mu'}(E)+\delta_{\nu\nu'}\delta_{\mu\mu'}\varepsilon_{\nu\mu}, \tag{35}$$

and $A_{\gamma\tau,\nu\mu}$ is the unitary matrix which diagonalizes the matrix U'. The function $z(E)$ is related to the phase shift Δ due to the configuration interaction of Ψ_E with the multiconfiguration bound components $\Phi_{\nu\mu}$, i.e.,[5]

$$\Delta(E)=-\tan^{-1}[\pi/z(E)]. \tag{36}$$

Substituting Eq. (36) into Eq. (32), the expansion coefficients $f_{\nu\mu}(E)$ are finally given by a simple expression

$$f_{\nu\mu}(E)=\cos\Delta(E)\zeta_{\nu\mu}(E). \tag{37}$$

With the expansion coefficients $a_{m(\varepsilon)l}$ and $f_{\nu\mu}$ in the final-state wave function Ψ_E given explicitly by Eqs. (18), (19), and (37), we now turn our attention to the calculation of the photoionization. The cross sections (in unit of a_0^2) in the dipole-length and dipole-velocity approximations are given, respectively, by

$$\sigma^L=\tfrac{4}{3}\pi^2\alpha E_\gamma|D^L_{Ei}|^2 \tag{38}$$

and

$$\sigma^V=\tfrac{16}{3}\pi^2\alpha E_\gamma^{-1}|D^V_{Ei}|^2, \tag{39}$$

where E_γ is the photon energy in rydberg units and α is the fine-structure constant. The dipole matrix D_{Ei} in the frozen-core approximation is given by

$$D_{Ei}=\langle\Psi_E|\hat{D}(1,2)|\Phi_i\rangle, \tag{40}$$

where

$$\hat{D}(1,2)=D(1)+D(2) \tag{41}$$

and D are the position and gradient operators for the length and velocity approximations, respectively.

A direct substitution of Eqs. (1), (18), (19), and (37) into Eq. (40) will separate the dipole matrix D_{Ei} into three terms, i.e.,

$$D_{Ei}(E)=D_1(E)+D_2(E)+D_3(E), \tag{42}$$

where

$$D_1=\cos\Delta\langle\psi_{ns\varepsilon_0 l}|\hat{D}|\Phi_i\rangle, \tag{43}$$

$$D_2=\cos\Delta\sum_{\nu,\mu}\zeta_{\nu\mu}(E)\langle\Phi_{\nu\mu}|\hat{D}|\Phi_i\rangle, \tag{44}$$

$$D_3=\cos\Delta\sum_{\nu,\mu}\zeta_{\nu\mu}(E)\langle\psi_{nsG^l_{\nu\mu}}|\hat{D}|\Phi_i\rangle. \tag{45}$$

The first term represents the direct transition from the initial state to the final $ns\varepsilon l$ background channel. The second term represents the contribution due to the transition from the initial state to the multiconfiguration bound components of the state wave function. The third term represents the contribution due to the interference between these two processes. The function $\psi_{nsG^l_{\nu\mu}}$ in Eq. (45) is exactly the same as the single configuration wave function $\psi_{ns\varepsilon l}$ except that the one-particle radial function $\chi_{\varepsilon l}$ in $\psi_{ns\varepsilon l}$ is replaced by the solution $G^l_{\nu\mu}$ of the inhomogeneous differential equation (27).

The advantage of the Fano procedure when applied to the photoionization dominated by the doubly excited autoionization state is clearly demonstrated by the separation of the strong and smooth energy-dependent parts into Eqs. (44) and (45), and Eq. (43), respectively. As shown by Eqs. (44) and (45), the energy dependence of the photoionization cross section is predominantly determined by the product of $\cos\Delta$ and $\zeta_{\nu\mu}$, which is subject to a large variation as the energy E moves across the energy eigenvalue $\varepsilon_{\gamma\tau}(E)$ in the energy denominator shown in Eq. (33). As pointed out by Fano,[5] at $\varepsilon_{\gamma\tau}$, the peak photoionization cross section corresponding to a doubly excited autoionization state dominated by the $n_\nu l_\nu n_\mu l_\mu$ configuration will remain finite. In fact, it can be shown readily that this peak cross section is inversely proportional to the width $\Gamma_{\nu\mu}$ of the autoionization state[5,9,15] and given approximately by

$$\sigma^{\max}_{\nu\mu}\sim|T_{\nu\mu}|^2/\Gamma_{\nu\mu}, \tag{46}$$

where

$$T_{\nu\mu}=\langle\Phi_{\nu\mu}|\hat{D}|\Phi_i\rangle+\langle\psi_{nsG^l_{\nu\mu}}|\hat{D}|\Phi_i\rangle. \tag{47}$$

With the strong energy dependence identified analytically, the entire photoionization spectrum of large energy variation can be carried out by interpolating numerically the calculated results at a small number of energy values.

Finally, we turn our attention to the calculation of the dipole matrices in Eqs. (43)–(45). First, for the D_1 term, the matrix element can be expressed as a sum of matrix elements of $\hat{D}$ between $\psi_{ns\varepsilon_0 l}$ and all single configuration wave functions $\psi_{n_1 l_1,n_2 l_2}$ included in the initial state wave function Φ_1, i.e.,

$$\langle\psi_{ns\varepsilon_0 l}|\hat{D}|\Phi_i\rangle=\sum_{n_1 l_1,n_2,l_2}C^{SL_i}(n_1 l_1,n_2 l_2)\times\langle\psi^{SL}_{ns\varepsilon_0 l}|\hat{D}|\psi^{SL_i}_{n_1 l_1,n_2 l_2}\rangle, \tag{48}$$

where following a straightforward application of angular momentum algebra, the matrix element of $\hat{D}$ between single configuration wave functions ψ is given by a general expression

$$\langle \psi^{SL}_{n_2'l_2',n_2l_2} \mid \hat{D} \mid \psi^{SL_i}_{n_1'l_1',n_1l_1} \rangle = (2L+1)^{1/2} T_{21} , \quad (49)$$

where

$$T_{21} = d(2'2,1'1;LL_i) + (-1)^S d(2'2,11';LL_i) + d(22',11';LL_i) + (-1)^S d(22',1'1;LL_i) \quad (50)$$

is the dipole transition matrix between configurations $(n_2'l_2',n_2l_2)$ and $(n_1'l_1',n_1l_1)$. For configurations with two equivalent electrons, a factor of $2^{-1/2}$ should be included in T_{21}. The matrix element d is the product of the angular coefficient ρ and the one-particle radial integrals, i.e.,

$$d(2'2,1'1;LL_i) = \rho(l_2'l_2l_1'l_1;LL_i) \langle \chi_{n_2l_2} \mid \chi_{n_1l_1} \rangle \times \langle \chi_{n_2'l_2'} \mid t \mid \chi_{n_1'l_1'} \rangle . \quad (51)$$

The angular coefficient ρ is given by

$$\rho(l_1l_2l_3l_4;L'L) = (-1)^{l_1} [(2l_1+1)(2l_3+1)]^{1/2} \begin{bmatrix} l_1 & 1 & l_3 \\ 0 & 0 & 0 \end{bmatrix} \times \begin{Bmatrix} L & 1 & L' \\ l_1 & l_4 & l_3 \end{Bmatrix} \delta_{l_2l_4} \quad (52)$$

and $\langle \chi_{n'l'} \mid t \mid \chi_{nl} \rangle$ is the one-particle radial dipole matrix where t is the radial part of the position and gradient operators in the length and velocity approximation, respectively.

Similarly, the matrix element in the D_2 term is given by

$$\langle \Phi_{\nu\mu} \mid \hat{D} \mid \Phi_i \rangle = \sum C^{SL}_{\nu\mu}(n_2'l_2',n_2l_2) C^{SL_i}(n_1'l_1',n_1l_1) \times (2L+1)^{1/2} T_{21} , \quad (53)$$

where the sum is taken over all configurations included in the multiconfiguration wave functions Φ_i and $\Phi_{\nu\mu}$. The matrix element in the D_3 term is exactly the same as the one given in Eq. (48) except that the radial wave function $\chi_{\varepsilon_0 l}$ is replaced by the solution $G^l_{\nu\mu}$ of the inhomogeneous equation (27).

III. PHOTOIONIZATION FROM THE Mg $3s3p\ ^1P$ TO THE $3p^2\ ^1S$ AUTOIONIZATION STATE

In this section we present a detailed photoionization cross-section calculation for the transition from the Mg $3s3p\ ^1P$ excited state to the ^1S continuum above the first ionization threshold dominated by the $3p^2\ ^1S$ doubly excited autoionization state. This process is chosen to demonstrate the effectiveness of the theoretical procedure outlined in Sec. II for the reason that both initial and final state of this transition are affected significantly by the configuration interaction. For example, our recent term value[10] and oscillator strengths[11] calculations have shown that the $3s3p\ ^1P$ state is mixed significantly with the $3pnd$ configuration series. As for the $3p^2\ ^1S$ state, our recent autoionization width calculation[15] has also demonstrated that it is mixed strongly with the $3s^2$ ground-state configuration. Experimentally, this transition is perhaps the best characterized photoionization process from an excited state of an alkaline-earth-metal atom. Although the absolute peak photoionization cross section for the $3p^2\ ^1S$ autoionization state is determined with an uncertainty of about 50% [i.e., $(8\pm4)\times10^{-16}$ cm^2], its width and line profile are well resolved by the earlier photoelectron measurement[2] and confirmed by the recent two-step laser experiment.[1] Theoretically, a detailed close-coupling calculation was performed by Thompson *et al.*[16] with a peak photoionization cross section of about 12.7×10^{-16} cm^2. Despite its reasonable agreement in cross section with the experiment, its calculated autoionization width is about a factor of 2 too small.

In the present calculation, the multiconfiguration state wave function Φ_i for the $3s3p\ ^1P$ initial state is calculated with exactly the same procedure we have employed in our recent term value and oscillator strengths calculations.[10,11] The same procedure is also employed for the calculation of the multiconfiguration bound components $\Phi_{\nu\mu}$ of the final-state wave function Ψ_E. Although a smaller number of configurations (e.g., 50–60 configurations) are sufficient for the numerical convergence up to four effective figures in energy eigenvalues, we have included a total of 149 configurations, excluding the bound part of the background open channel $3sn(\geq4)s$, in the calculation of $\Phi_{\nu\mu}$. In particular, since the $3s^2\ ^1S$ ground state is mixed strongly with the $3p^2\ ^1S$ autoionization state, its contribution to the Ψ_E is included in the $\Phi_{\nu\mu}$ terms instead of the background open channel represented by the first two expansion terms in Eq. (1). Such a choice has the effect of transferring the interaction strength between the $3p^2$ and $3s^2$ configurations from an approximated second-order perturbation contribution into a nonperturbative bound component through the diagonalization of the Hamiltonian matrix in the SCW procedure. Finally, we note that only a limited number (e.g., varied from 9 to 17 in this application) of multiconfiguration bound components $\Phi_{\nu\mu}$ representing the $3pnp\ ^1S$ and other higher doubly excited autoionization states as well as the $3s^2$ ground state are required in the third expansion term in Eq. (1). A value of $\alpha=0.489$ a.u. for the static core dipole polarizability[17] and $r_0=1.1683a_0$ for the cutoff radius are chosen for the present calculation so that the correct $3p$ series limit is reproduced.

The calculated photoionization cross sections as functions of wavelengths in the dipole-velocity and dipole-length approximations are shown in Fig. 1. A total of 17 multiconfiguration bound components $\Phi_{\nu\mu}$ are included. The peak cross sections calculated in the velocity and length approximations are 4.67×10^{-16} cm^2 and 4.66×10^{-16} cm^2, respectively. The peak cross section is reduced slightly if the number of $\Phi_{\nu\mu}$ included in Ψ_E is also reduced. For example, the peak cross section in the dipole-velocity approximation is reduced to 4.31×10^{-16} cm^2 when the number of $\Phi_{\nu\mu}$ is reduced to 9, as shown in Fig. 2. Regardless the number of $\Phi_{\nu\mu}$ included in Ψ_E, the velocity and length results remain in good agreement with each other at energies close to the center of the autoionization state.

The effect of the second-order perturbation contribution, represented by the D_3 term, is relatively large in the length calculation. As shown in Fig. 3, the peak cross

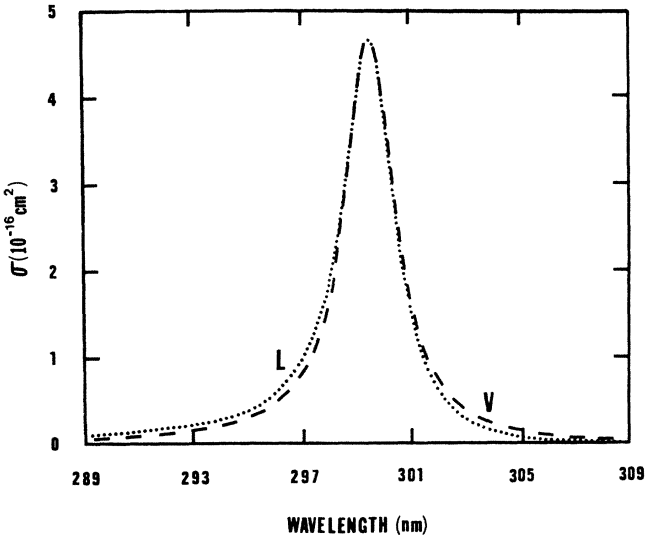

FIG. 1. Calculated photoionization cross sections σ (10^{-16} cm^2) in dipole-velocity (dashed curve V) and dipole-length (dotted curve L) approximations as a function of wavelength λ (in nanometers). A total of 17 multiconfiguration bound components $\Phi_{\nu\mu}$ are included in the state wave function Ψ_E.

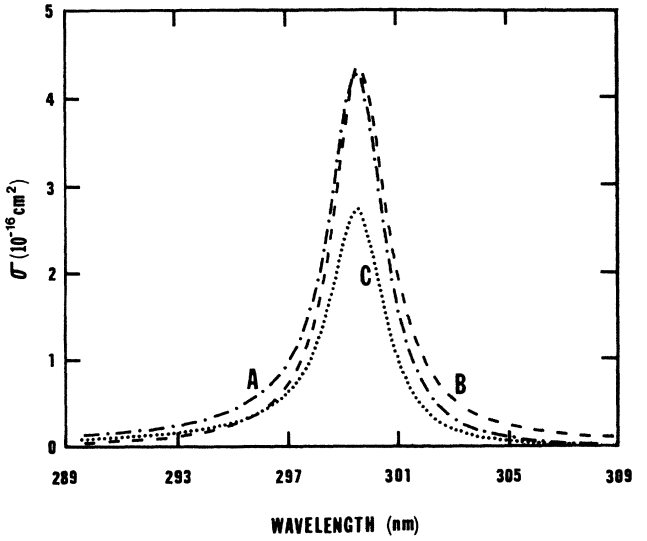

FIG. 3. Comparison between the calculated dipole-length photoionization cross sections σ (10^{-16} cm^2) as a function of wavelength λ (in nanometers) with contribution from different combinations of D_1, D_2, and D_3 terms. A (dashed-dotted curve) represents the cross section with all three terms included. B (dashed curve) represents the cross section with D_1 excluded and C (dotted curve) represents the cross section with D_3 excluded.

section is reduced to 2.71×10^{-16} cm^2 from a value of 4.29×10^{-16} cm^2 when the contribution from D_3 term is excluded from the dipole matrix D_{Ei}. The contribution from the direct transition, represented by the D_1 term, is smaller but still noticeable in the length calculation. This effect is illustrated in Fig. 3 as the cross sections are increased on the longer wavelength side and decreased on the shorter wavelength side when the contribution from the D_1 term is excluded from the dipole matrix D_{Ei}. In contrast, our velocity calculation has shown that the contributions from both D_1 and D_3 terms are negligible.

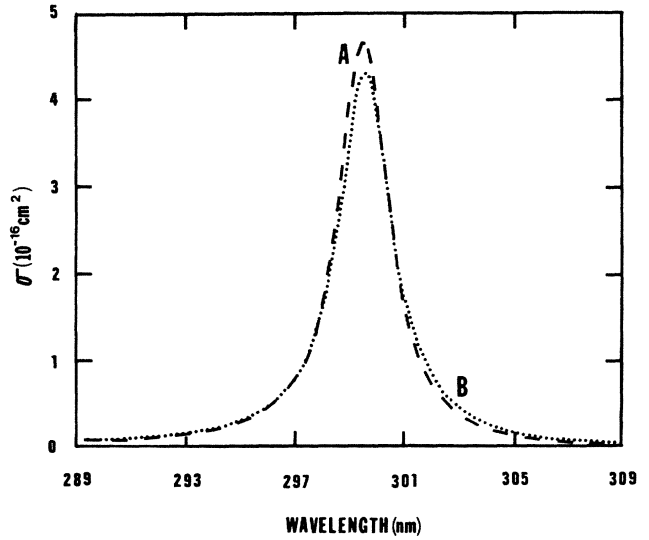

FIG. 2. Comparison between the calculated photoionization cross sections σ (10^{-16} cm^2) in the dipole-velocity approximation as function of wavelength λ (in nanometers) between calculations with the number of multiconfiguration bound components $\Phi_{\nu\mu}$ equal to 17 (dashed curve A) and 9 (dotted curve B), respectively.

The results of the present calculation are in close agreement with the available experimental data. In particular, the calculated width[15] of 271 cm^{-1} is in excellent agreement with the experimental widths of 278±8 cm^{-1} from the two-step laser experiment[1] and 276±11 cm^{-1} from the photoelectron experiment.[2] The peak cross section for the $3p^2\,{}^1S$ autoionization also agree well with the experimental value from the photoelectron measurement. Although it appears that the present calculated peak cross section is substantially smaller than the close-coupling results of Thompson *et al.*,[16] the dipole matrix D_{Ei} in the present calculation is only approximately 10–20 % smaller than the close-coupling results. This can be seen readily from the scaling of the peak cross section in Eq. (48); $\sigma^{\max}$ is inversely proportional to the width Γ, which is a factor of 2 too small than the correct value in the close-coupling calculation.

In conclusion, by including explicitly the multiconfiguration bound components dominated by the doubly excited autoionization states in the state wave function Ψ_E, we have demonstrated that the configuration-interaction approach developed by Fano[5] can be applied effectively in the quantitative determination of the photoionization cross sections for transitions dominated by the strong multielectron interaction for a quasi-two-electron atom. The success of this calculational procedure also relies on the ability to identify the strong configuration in-

teraction between bound configurations. Finally, we note that the computational effort required in the application of the theoretical procedure represented in Sec. II is quite modest and all numerical results reported in Sec. III are performed with a desktop personal computer.

ACKNOWLEDGMENTS

This work is supported by the National Science Foundation under Grant No. PHY84-08333. Many interesting discussions with Dr. X. Tang are also acknowledged.

[1]R. E. Bonanno, C. W. Clark, and T. B. Lucatorto, Phys. Rev. A **34**, 2082 (1987).
[2]D. J. Bradley, C. H. Dugan, P. Ewart, and A. F. Purdie, Phys. Rev. A **13**, 1416 (1976).
[3]For example, D. Rassi, V. Pejcev, T. W. Ottley, and K. J. Ross, J. Phys. B **10**, 2913 (1977); S. Trajmar, in *Electronic and Atomic Collisions,* edited by G. Watel (North-Holland, New York, 1978), p. 113.
[4]For example, J. P. Press, C. E. Burkhardt, W. P. Carver, and J. J. Leventhal, Phys. Rev. A **29**, 985 (1984); W. Fiedler, Ch. Kortenkamp, and P. Zimmermann, *ibid.* **36**, 384 (1987).
[5]U. Fano, Phys. Rev. **124**, 1866 (1961).
[6]G. Bates and P. L. Altick, J. Phys. B **6**, 653 (1973).
[7]P. L. Altick and E. N. Moore, Phys. Rev. **147**, 59 (1966).
[8]T. N. Chang and Y. S. Kim, Phys. Rev. A **34**, 2609 (1986).
[9]T. N. Chang, Phys. Rev. A **34**, 4554 (1986).
[10]T. N. Chang, Phys. Rev. A **34**, 4550 (1986).
[11]T. N. Chang, Phys. Rev. A **36**, 447 (1987).
[12]C. Bottcher and A. Dalgarno, Proc. R. Soc. London, Ser. A **340**, 187 (1974).
[13]A. R. Edmonds, *Angular Momentum in Quantum Mechanics* (Princeton University Press, Princeton, NJ, 1957).
[14]T. N. Chang and R. T. Poe, J. Comput. Phys. **12**, 557 (1973).
[15]T. N. Chang, Phys. Rev. A **36**, 5468 (1987).
[16]D. G. Thompson, A. Hibbert, and N. Chandra, J. Phys. B **7**, 1298 (1974).
[17]U. Opik, Proc. Phys. Soc. London **92**, 566 (1967).